PRAMANA
— journal of
physics

Vol. 80, No. 4
April 2013
pp. 685–699

Arc plasma devices: Evolving mechanical design from numerical simulation

S GHORUI* and A K DAS
Laser and Plasma Technology Division, Bhabha Atomic Research Centre, Trombay, Mumbai 400 085, India
*Corresponding author. E-mail: srikumarghorui@yahoo.com

MS received 23 January 2012; revised 24 September 2012; accepted 8 October 2012

Abstract. Wide ranges of technological applications involve arc plasma devices as the primary plasma source for processing work. Recent findings exhibit the existence of appreciable thermal non-equilibrium in these so-called thermal plasma devices. Commercially available magnetohydrodynamic codes are not capable of handling such systems due to unavailability of non-equilibrium thermodynamic and transport property data and self-consistent models. A recipe for obtaining mechanical design of arc plasma devices from numerical simulation incorporating two-temperature thermal non-equilibrium model is presented in this article with reference to the plasma of the mixture of molecular gases like nitrogen and oxygen. Such systems are technologically important as they correspond to the plasma devices operating with air, oxygen plasma torches in cutting industries and plasma devices using nitrogen as shielding gas. Temperature field, associated fluid dynamics and electrical characteristics of a plasma torch are computed in a systematic manner to evaluate the performance of a conceived design using a two-fluid CFD model coupled with a two-temperature thermodynamic and transport property code. Important effects of different nozzle designs and plasma gases obtained from the formalism are discussed. Non-equilibrium thermodynamic properties are computed using modified two-temperature Saha equations and transport properties are computed using standard Chapman–Enskog approach.

Keywords. Arcs; air plasma; plasma torch; non-equilibrium plasma; plasma simulation; torch design.

PACS Nos 52.50.Nr; 52.30.Ex; 52.50.Dg

1. Introduction

Arc plasma devices serve as the key components for numerous technological applications [1]. Processes like synthesis of nanostructures [2,3], disposal of toxic ash, waste, asbestos containing material [4], vitrification and calcination of radioactive wastes, reduction of radioactive halides, recovery of metals like zinc, aluminium, iron from wastes or ores, melting of steel scrap, sponge iron, zirconium [5,6], decomposition of nitrate, cracking of

DOI: 10.1007/s12043-012-0491-2; ***e*Publication: 24 March 2013**

hydrocarbon, defluorination of phosphates, surface modification through plasma nitriding [7], diamond film deposition, thermal barrier coatings [8,9], biomedical decontamination [10], plasma treatment of fibres [11] etc. are some important areas of application. A plasma-generating device, known as plasma torch, serves as the basic unit for plasma generation in all such applications. These plasma sources are characterized by their high enthalpy content, high temperature (10,000–50,000 K), wide ranges of operating power (kW to MW) and a large combination of working gases. Initially, such devices were built based on the experienced behaviour without knowing much about the physical process happening inside. Impact of various physical processes on the overall performance of the device was not clear. Attempts were made to understand such devices through equilibrium simulations assuming the plasma to be in thermal equilibrium [12–18]. However, experimental observations and subsequent theoretical studies indicated the presence of thermal non-equilibrium in such devices and non-equilibrium modelling received a huge boost in recent years [19–23]. The present paper reports the evolving mechanical design of such arc plasma devices from two-temperature non-equilibrium modelling.

Schematic of a generic plasma torch and its operation is shown in figure 1. The gas enters through a tube in the cylindrical space between the cathode and the anode. On its way towards anode it meets an established arc between the electrodes and gets heated to generate plasma. The plasma finally comes out from the anode exit in the form of a plasma jet for process application. Usually, a constant current DC power supply continuously feeds power into the system for sustained operation.

Depending on the application, plasma torches vary widely in design, power, size and robustness. Past decades have seen remarkable efforts in the design and development of plasma torches both in the private sectors around the globe as well as in the government organizations [24–28]. A rapid growth in research and development has led to

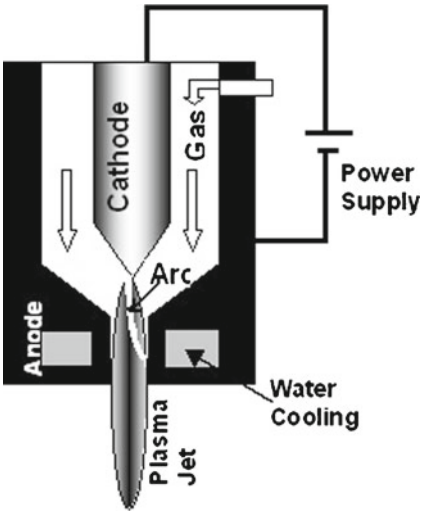

Figure 1. Schematic of a plasma torch and its operation.

better understanding of the plasma state, discovery of better electrodes, finding of superior insulators, better manufacturing techniques for complex components and development of more rugged and compact plasma devices.

Over the last two decades, understanding about the physical processes improved significantly through easily available computational resources and innovative experiments [12–28]. Numerical simulation gained huge momentum to assist design and development of these unique heat-generating devices [12–18]. Cathode and anode design, associated heat transfers, arc diameter, arc stabilization, heat-flux profiles, plasma temperature distribution, velocity profiles, device efficiency, spatial concentration of nascent active species and effect of gas properties on design parameters are some of the thrust areas where simulation has great potential to serve as a unique tool for quick information on design considerations without actually building the device. As these devices are prone to thermal non-equilibrium and the fact that thermodynamic and transport properties vary drastically with degree of thermal non-equilibrium, state-of-the-art modelling approach employs two-temperature fluid dynamic modelling of the flowing plasma with appropriate boundary conditions. While mixtures of molecular gases like nitrogen and oxygen are technologically important as the major constituents of air plasma, no such modelling work is done for torches using such gases. In an effort to establish this approach as a state-of-the-art design tool for such gases, evolving mechanical design of a solid cathode plasma torch from numerical simulation is presented in this article.

2. Heat transfer to the electrodes

The most important design consideration in fabricating a plasma torch is the heat transfers to the cathode and the anode. Inadequate cooling of the electrodes may severely limit the lifespan of a plasma source by rapid erosion of the electrodes, failing of brazing joints, melting and evaporation of the electrodes, and puncturing of the electrode wall. In a typical non-transferred arc plasma torch, around half of the electrical input power goes as thermal heat load to the torch components. While cathode is subjected to only 1–5% of this heat load, the anode shares a major part of the remaining heat load. It has been observed experimentally that higher the torch power lesser is the percentage of heat load received by the cathode.

2.1 *Cathode heat transfer*

Mechanism of cathode heat transfer is illustrated in figure 2. Primary heating mechanism for the cathode is the Joule heating which is a function of cathode diameter and the current passing through it. Other components that may contribute towards heating mechanism are the radiation from the bulk plasma and the ion bombardment. Radiation from the hot cathode tip to the surrounding cold gas may also have a cooling effect. However, the effects of the latter two are insignificant compared to the first one.

A cathode serves its basic purpose inside a plasma torch by emitting copious electrons through thermionic and field emissions. While the first one depends on the temperature (T_K) of the emitting surface, the second one depends on the prevailing electric field (E_K).

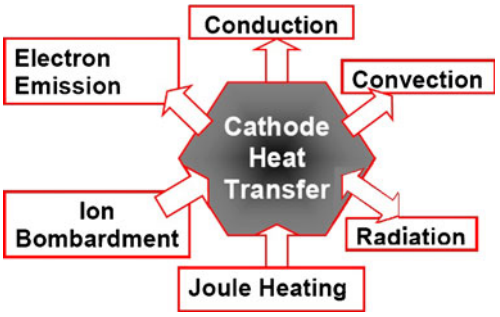

Figure 2. Mechanism of cathode heat transfer.

The well-known Richardson–Schotky equation predicts the current density at the cathode surface as

$$J = AT_{\mathrm{K}}^2 \exp\left[-e\left(\frac{\Phi_{\mathrm{K}} - \sqrt{\frac{eE_{\mathrm{K}}}{\pi\varepsilon_0}}}{k_{\mathrm{B}}T_{\mathrm{K}}}\right)\right], \tag{1}$$

where A is a constant, Φ_{K} is the work function of the cathode, k_{B} is the Boltzmann constant, e and ε_0 are the electronic charge and permittivity of free space. Higher the temperature and higher the electric field, higher is the emission current density. However, excessive heating causes melting of the electrode and additional cooling becomes compulsory in most of the design considerations for the integrity of the cathode.

Conduction, convection and electron emission are the basic cooling mechanisms associated with the cathode of a plasma torch. Depending on the cathode material, a large part of the generated heat is conducted away to the reservoir of cooling water. Usually the cathode and the gas injection sections are designed in such a way that after entering through the inlet port, cold plasma gas flows over the hot cathode surface before finally entering into the arc region. Significant convective heat transfer of the cathode takes place in the process. Also, electrons, in equilibrium with the hot cathode surface, impart cooling effect as they take away the energy with it when emitted.

Therefore, while cooling is necessary for the integrity of the cathode, an elevated temperature is a requirement for proper emission. Best performance requires securing an optimum cooling design.

2.2 *Anode heat transfer*

Similar to cathode conduction, convection, Joule heating, radiation and electronic heat transfer are the major heat transfer mechanisms for the anode (figure 3). However, as anode plays a role different from that of the cathode, the mechanisms contribute in a different manner.

Unlike cathodes, convection now acts as a strong agent for anode heating. The cool gas, after passing over the cathode, enters the arc zone and experiences severe thermal abuse by the electric arc. It expands, ionizes and forms plasma. Depending on the internal

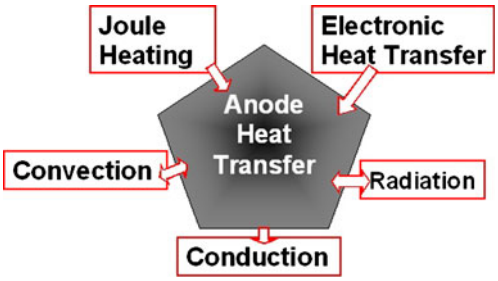

Figure 3. Mechanisms of anode heat transfer.

profiling of the flow channel, the extremely hot expanding plasma gas collides with the wall resulting in convective heat transfer. The heat transfer depends on the alignment of the cathodes with respect to the axis of the flow channel and usually a cool boundary layer in touch with the anode limits the amount of heat transferred to the wall. Any misalignment may cause puncturing of the boundary layer and a sharp rise in the anode heat transfer by convection.

Usually, thick copper walls are maintained in most of the anode designs in arc plasma devices. As a result, a very low resistance path is offered for the arc current to pass through. Therefore, unlike cathode there is no significant bulk Joule heating of the anode. However, the mechanism contributes significantly at the location of the anode arc spot where formation of arc root takes place. Because of the small size of the spot, the heating may be intense enough to cause melting and eventual puncturing of the anode wall.

Electronic heat transfer is a very significant mechanism when anode heat transfer is considered at the arc spot. There are three components of this: thermal energy of the electrons, energy gained from the electric field and energy released when an electron is absorbed in the wall. Associated heat transfer may be described as

$$Q_{\mathrm{el}} = J\frac{5k_{\mathrm{B}}T_{\mathrm{e}}}{2e} + JV + J\varphi, \tag{2}$$

where V is the arc voltage and φ is the work function of the anode material. The first terms gives the thermal energy of the electrons, the second terms give energy gained from the electric field and the last terms represent the energy released when the electrons become a part of the anode wall. It may be noted that each of these terms is linearly proportional to the current density. Therefore, this part of the anode heat transfer is strongly dependent on the sustained arc current.

Because of the extremely high temperature of the inner plasma core, anode wall receives significant amount of heat through radiation. Part of this radiated heat from the inner core is reflected back into the plasma by the inner wall of the anode. Also, the outer part of the anode exposed to atmosphere radiates heat to the surrounding. Net effect of anode heating due to radiation is thus usually small compared to other sources.

Heat, deposited over the anode, is taken away by the coolant in the cooling channel designed within the anode. Conduction is the primary mechanism to take away

this heat to keep the temperature of the anode below the melting point of the anode material.

2.3 *Incorporating heat transfer mechanisms in the numerical model*

Considering relative contributions from different heat transfer mechanisms and associated computational complexities to incorporate them in a model, a number of simplifying assumptions are made in this study to get a fast but appreciably accurate estimate of the plasma quantities using a 2D model. While the computational domain incorporates the solid parts of the torch, coolant channels embedded in these parts are complex and asymmetric and cannot be directly incorporated in a 2D simulation model. However, experimentally it has been observed that the cooling system is capable of maintaining nearly a steady temperature over the inner wall of the anode, and variation of this temperature along the length of the intensely cooled electrode is small compared to the temperature scale of interest. Based on measurement, a fixed temperature boundary condition is used at the inner wall of the anode and cooling loop details inside the solid parts of the electrodes are excluded. As current passes through the anode, it heats it up through ohmic heating but the path followed by the current through the anode remains undetermined and therefore, making a correct estimate of the associated ohmic heating is difficult. However, owing to the extremely low resistance of the thick copper anode, resistive heating involved is small compared to the other competing sources and is not included in the study. For radiative energy transfer, it has been assumed that whatever radiation falls on the inner surface of the anode is lost and is not reflected back into the system. Formation of arc spot is inherently asymmetric and cannot be incorporated in a 2D model. Associated heat transfer described by eq. (2) is not considered. The simulation is therefore most appropriate for transferred arc mode operations where the arc is transferred to a job outside and no current flows towards the anode wall, or for cases of non-transferred arcs where the arc comes out from the nozzle and makes a loop outside and finally reconnects at some point over the outer part of the nozzle. The second case is observed through fast photography in many torches having short nozzle sections [29]. Conduction and convection are the most dominating heat transfer mechanisms and are appropriately included in this study. For cathode, the temperature boundary conditions over the surface are derived from experimental observations. Associated radiation from the cathode tip, electron emission and ion bombardment contributions are not considered.

3. Obtaining mechanical design from numerical simulation

3.1 *The numerical model and the solution procedure*

For numerical simulation of the arc plasma devices, the plasma is assumed to be composed of two interpenetrating fluids, namely the electrons and the heavy particles. The two fluids are in equilibrium individually but are not at identical temperatures. At a given location, the electron fluid is characterized by the temperature, T_e, while the rest of the particles are characterized by a different temperature, T_h (usually lower than or equal to T_e). Energy

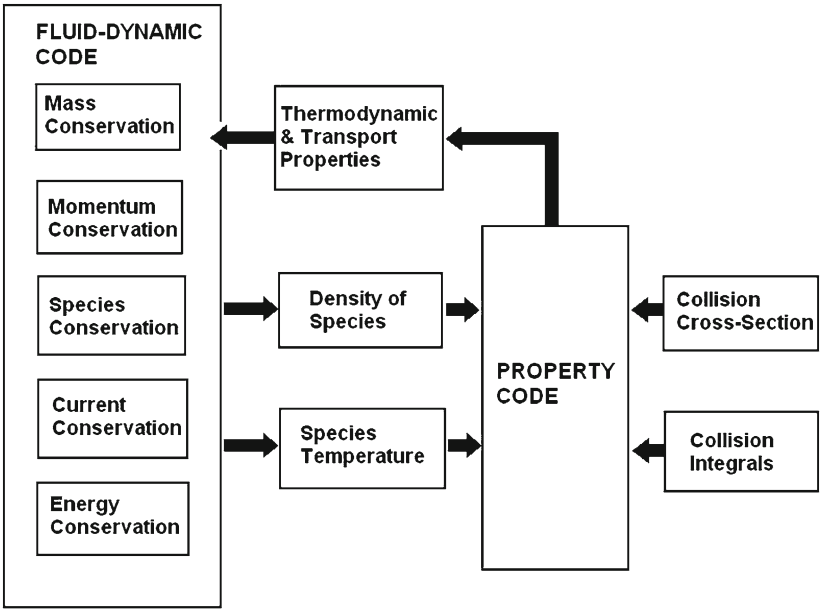

Figure 4. Numerical scheme used for the simulation.

exchange between these two fluids takes place through collisional mechanisms. Degree of non-equilibrium is described by the parameter T_e/T_h. The fluids are described by the associated Navier–Stokes equations for mass, momentum and energy conservations as described in detail in ref. [26].

Plasma composition and thermodynamic properties are computed using two-temperature Saha equation employing the latest energy level listing by NIST. Transport properties of the plasma under different non-equilibrium conditions are rigorously computed from the solution of the Boltzmann equation using the Chapman–Enskog's approach [22,30,31]. Associated collision integrals and cross-sections are taken from a recent compilation by Capitelli [32,33].

A schematic of the numerical scheme used in the simulation is presented in figure 4. The complete simulation is carried out through mutual interaction between two modules. The property code receives the density of species and species temperatures information from the fluid dynamic module and computes associated thermodynamic and transport properties with the help of collision integral, cross-section and energy level information stored. Once the property information is made available to the fluid dynamic code it starts solving the conservation equations to obtain plasma field quantities. A SIMPLE [34] like algorithm is used for solving the fluid dynamic part in an iterative manner under laminar flow conditions. Finite volume approach, used to discretize the system of equations, and the boundary conditions for the simulation are the same as those in ref. [21]. Updated density and species temperatures are then passed to the property code to update the property values and the process continues until the solution converges.

Table 1. Design parameter specifications.

Design parameter	Value	Design parameter	Value
Hafnium insert diameter	4 mm	Anode inner straight part	8.6 mm
Hafnium insert length	3 mm	Nozzle exit diameter	5 mm
Anode outer core diameter	30 mm	Nozzle length	7 mm
Anode inner core diameter	19 mm	Cathode tip angle	78°
Anode inner core angle	78°	Cathode diameter	12 mm
Anode outer profile angle	57.2°	Cathode straight top part	10 mm
Anode outer straight part	14 mm	Cathode length	13 mm

3.2 *Designing a torch*

A dedicated grid generator code is developed for easy design and for the modifications of plasma torch components and for the generation of associated finite volume grid for fluid dynamic simulation. Once the design parameters are specified as in table 1, design of the torch and the associated grid for the simulation is immediately generated by the code as in figure 5. An internal mesh control section of the code handles modification and refinement of the generated meshes as per requirement to facilitate convergence of the program. The torch internals and the finite volume mesh generated by the grid generator for the design parameters of table 1 are presented in figure 5. The cathode contains a

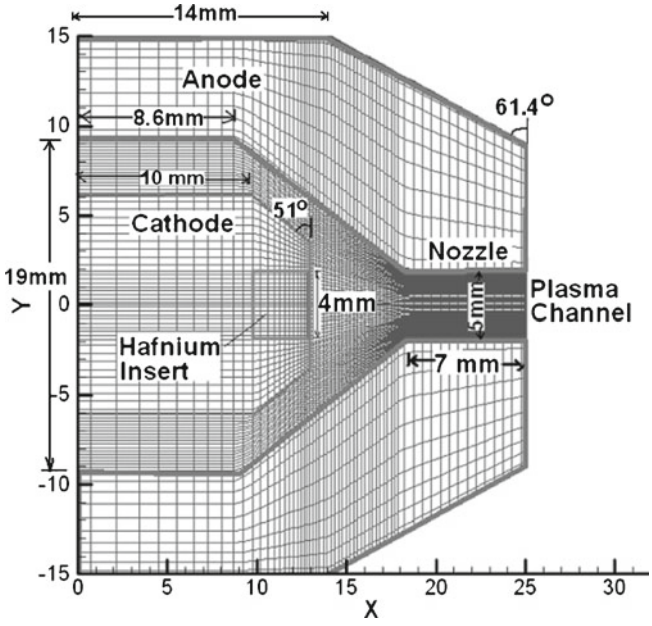

Figure 5. Geometry of the torch and the corresponding finite volume mesh as generated by the grid generator code according to the design specifications of table 1.

hafnium insert at the bottom to keep the cathode enabled emitting electrons in oxidizing environment.

3.3 *Device characteristics from numerical simulation*

The electrical, thermal and fluid dynamic characteristics as obtained from the numerical simulation of the plasma torch, designed in §3.2, are presented in this section. The idea is to understand the important characteristics like flow fields, temperature fields, efficiency etc. obtainable from the torch and to check if they meet our requirement. If not we need to modify the design in an intuitive manner and repeat the simulation for improving the device characteristics. It must be mentioned that the design chosen is a typical one and the same methodology can be applied to any modified design. Some such examples are given in the later part of this article.

Device characteristics obtained from the simulation are presented in figure 6. Distribution of temperature, electric potential, electron number density, plasma pressure, axial velocity and current density are presented in figures 6a–6f. The lower and upper parts of the temperature distributions in figure 6a represent the temperatures of the heavy particles and the electrons respectively. A more vivid variation of the field quantities is presented in figure 7. Radial variation of plasma temperature at the exit in figure 7a not only shows the existence of extremely high temperature but also shows that electron temperature remains always higher than the heavy particle temperature. The difference is less in the core and more near the boundary wall. The existence of such high non-equilibrium near the wall is believed to play an important role in current transfer to the anodes of arc plasma devices. Higher is the collision rate, better is the achievement of LTE. For a given pressure, when T_e increases, the collision frequency first increases and then decreases. The decrease is due to a drop in the number of particles per unit volume. The observed deviations from LTE at very high temperature axial regions (near the cathode and inside the nozzle) are caused by this. It may be noted that good LTE is observed along the axis in the zones in between the cathode and the nozzle.

Axial variation of electric potential presented in figure 7b is a direct check of reliability of any numerical model. Performing actual experiments, the model used has been tested to predict correct potential drop within the device in a number of designs. Figures 6c and 6d present distribution of electrons and pressure inside the plasma torch. Electronic and ionic populations in the emanating plasma jet are extremely important as far as active species-induced reactions are concerned. Axial variation of pressure within the torch is presented in figure 7d. As the cold gas enters into the arc zone, it expands, gets ionized and forms plasma. A rise in pressure in front of the cathode tip is observed for this. After this zone, the pressure starts droping almost linearly and reaches near atmospoheric pressure at the nozzle exit. Velocity of the exiting plasma jet (figure 6e) determines the length and radial extent of the outside plasma jet and the degree of impact with a job, kept in front of it for processing works like plasma spraying or plate cutting. Quality of the processing works depends to a large extent on these parameters. Radial variation of axial velocity at the torch exit, presented in figure 7c, indicates extremely high speed of the plasma jet for the nozzle design considered. Figure 6f presents the distribution of current density inside the plasma torch.

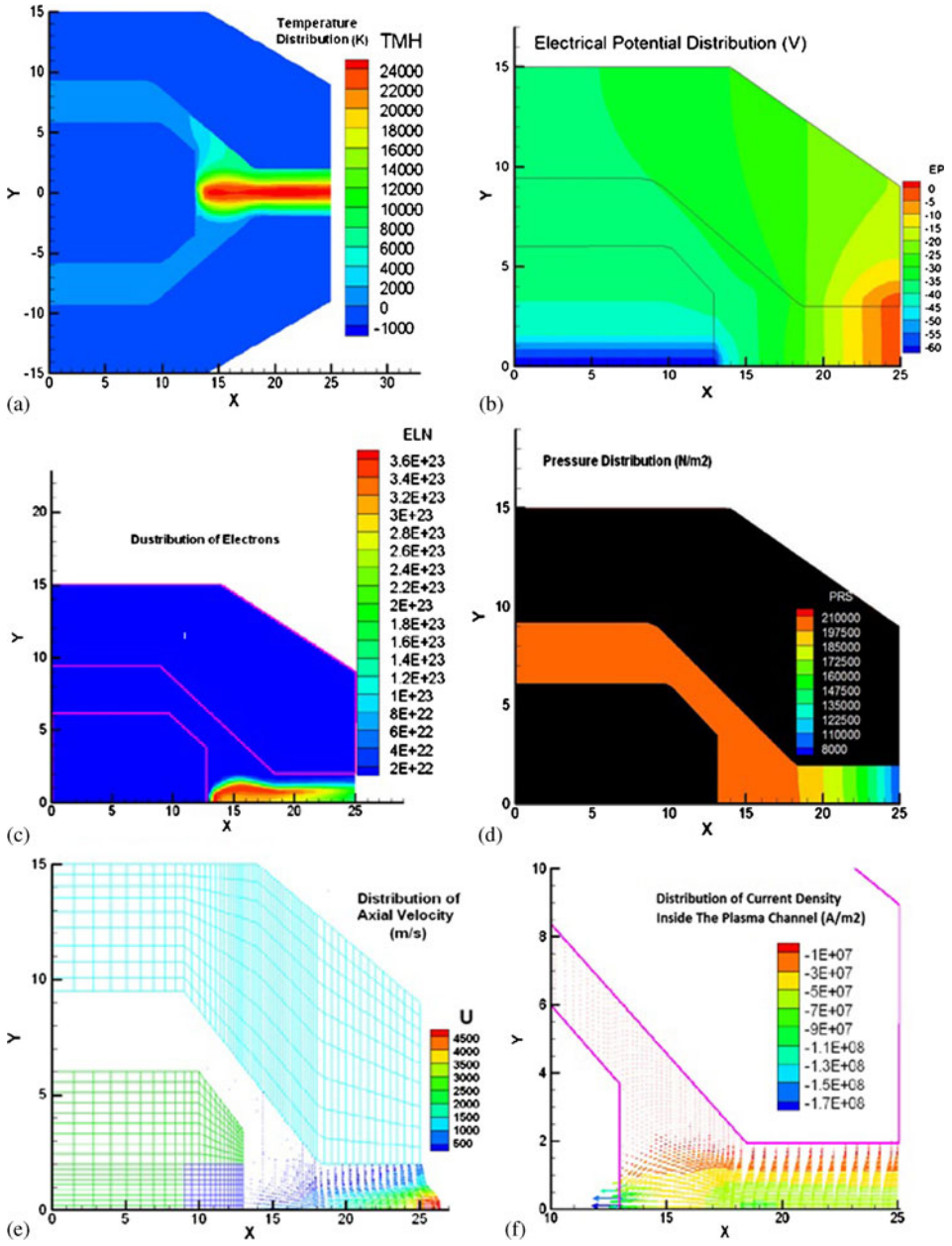

Figure 6. Device characteristics from simulation: (**a**) Distribution of temperature inside the plasma torch (lower part – heavy particle temperature and upper part – electron temperature), (**b**) distribution of electric potential, (**c**) distribution of electrons, (**d**) distribution of plasma pressure, (**e**) distribution of velocity vectors and (**f**) distribution of current density.

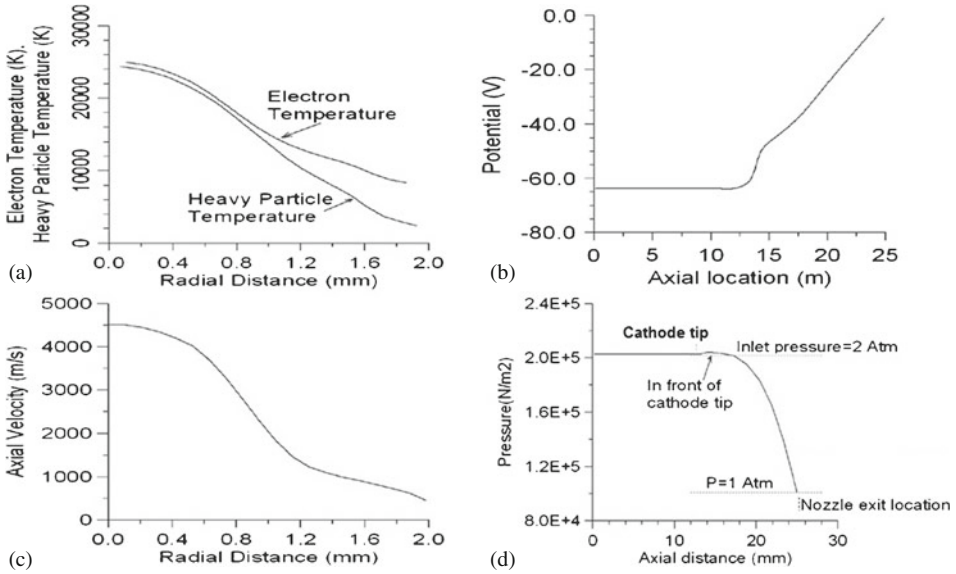

Figure 7. Variation of field quantities in the plasma jet: (**a**) Radial variation of electron and heavy particle temperature at the nozzle exit, (**b**) axial variation of electric potential, (**c**) radial variation of axial velocity at the exit and (**d**) variation of plasma pressure along the central axis of the torch.

Efficiency of a plasma torch is defined as the percentage of total electrical power available with the exiting plasma jet:

$$\text{Eff} = 2\pi \frac{\int_0^R \rho u h r \mathrm{d}r}{V_{\text{arc}} I_{\text{arc}}} \times 100\%, \tag{3}$$

where R is the radius of the nozzle exit, ρ, u and h correspond to density, axial velocity and enthalpy respectively. Rest of the electrical power is lost in cooling of different components of the device. Once the simulation reach a converged state, the computed

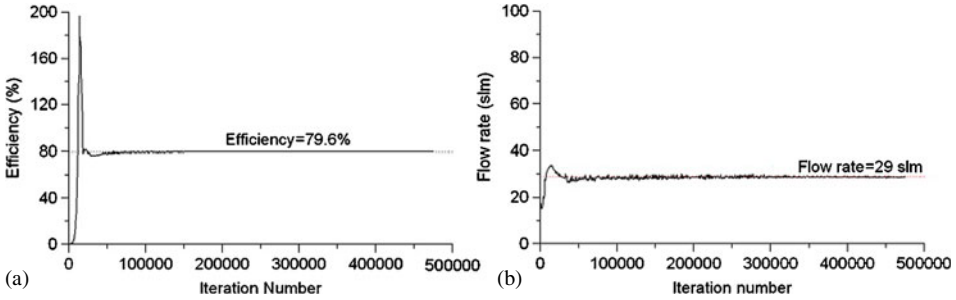

Figure 8. (**a**) Efficiency of the plasma torch as solution converges. (**b**) Flow rate of the outgoing plasma gas.

Table 2. Operational torch parameters from simulation for the chosen design and arc current.

Torch parameter	Simulated value	Torch parameter	Simulated value
Torch power	25.6 kW	Efficiency	79.6%
Arc current	400 A	Exit gas velocity	Parabolic with peak at 4500 m/s
Arc voltage	64 V	Anode heat flux	1.5 kW/cm^2
Anode heat load	5 kW	Cathode heat flux	0.8 kW/cm^2
Cathode heat load	300 W	Operating gas	Nitrogen 80% + Oxygen 20%

efficiency of the device and the net outflow of plasma gas reach a steady state as presented in figures 8a and b respectively. It is seen that the device designed is capable of offering efficiency as high as 79.6% for a flow rate around 29 standard litre per minute (slpm) of N_2–O_2 mixture in the ratio of 80 : 20. It has been observed from simulation that the efficiency of the torch decreases fast with increase in the anode channel length. For a given flow rate, arc current and geometry, the mean length of the arc during operation does not vary much. However, additional electrodes (like auxiliary anode, additional segments etc.) are sometimes unavoidable for high-frequency ignition of the arc and subsequent fluid dynamic stabilizations of the jet (especially for bigger sizes of the anode bore), resulting in longer channel length and subsequent reduction in efficiency. The longer the anode channel length, higher is the surface area for the loss of power to the coolant and lesser is the efficiency.

Operational parameters of the torch so obtained from the simulation are summarized in table 2. The obtained anode heat load of 5 kW is mainly distributed over the nozzle area and gives an average anode heat flux of 1.5 kW/cm^2. The average cathode heat flux is much less and computed as 0.8 kW/cm^2. The figures are well within the bearable limit of the electrodes. For very high power torches, diameter of the plasma channel should be increased appropriately to keep the wall heat flux low so that melting of the electrode does not take place.

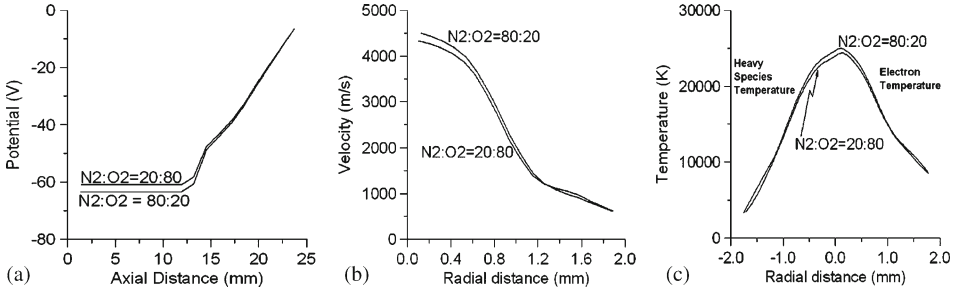

Figure 9. Effect of changing composition of plasma gas on torch characteristics: (**a**) Axial potential variation, (**b**) velocity distribution at the exit and (**c**) temperature distribution at the exit.

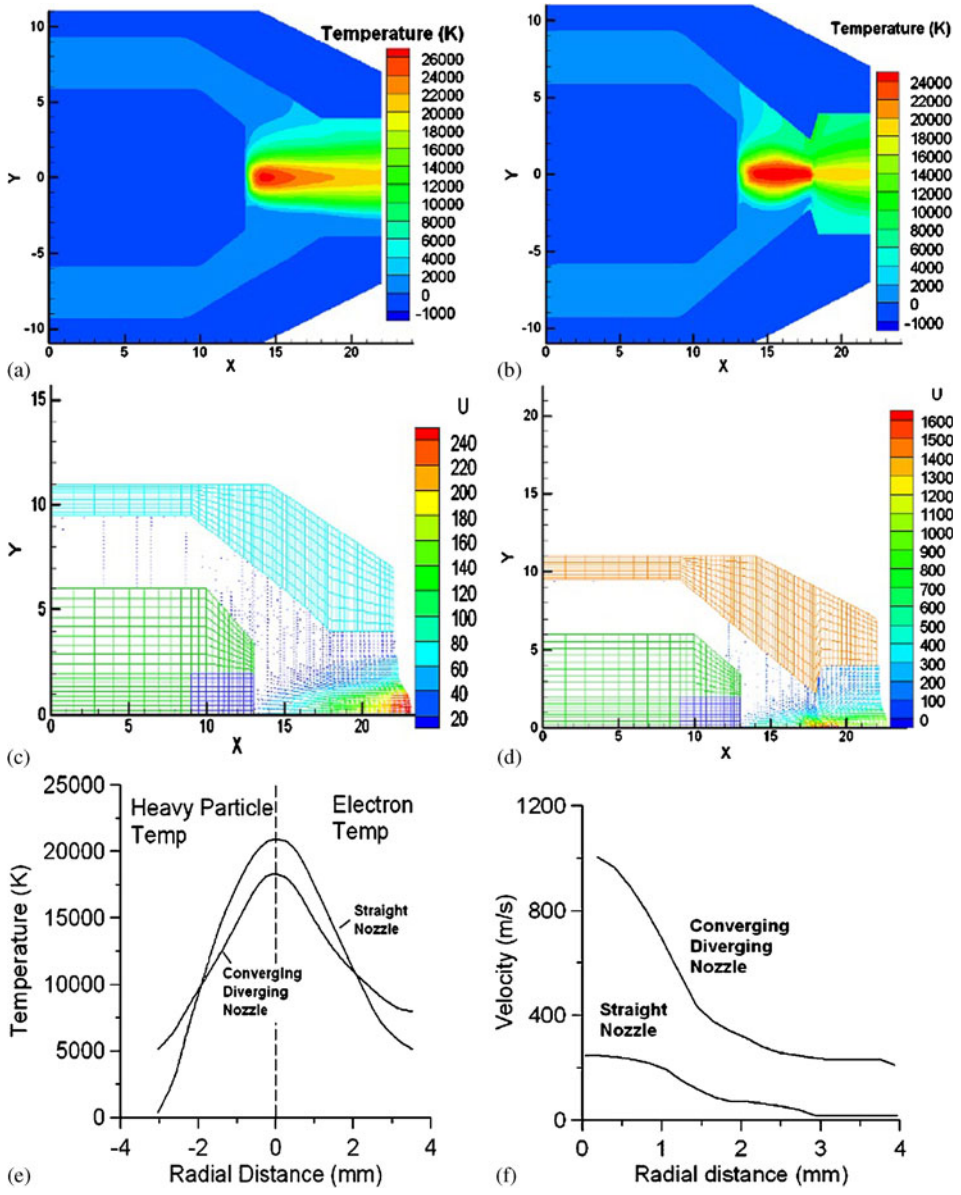

Figure 10. Simulated results for a straight nozzle and a Laval nozzle torch of the same exit diameter and operating at the same arc current (400 A) and with same plasma gas (N_2–O_2 mixture at a ratio of 80 : 20): (**a**) Temperature field for straight nozzle, (**b**) temperature field for Laval nozzle, (**c**) flow field for straight nozzle, (**d**) flow field for Laval nozzle, (**e**) comparison of exit temperature distribution and (**f**) comparison of exit velocity distribution.

3.4 *Torch design and the effect of plasma gases*

Operation of a torch and its characteristics are highly dependent on the type of gas used in generating the plasma. There is a huge difference in thermal and fluid dynamic characteristics of a plasma torch for monatomic and diatomic gases. Translational, rotational and vibrational degrees of freedom of diatomic gases result in higher specific heat compared to monatomic species having only translational degree of freedom. Wide variation in the behaviour results from the specific heat that bears a highly nonlinear variation with rise in temperature. However, if two diatomic gases are used and their ratios are changed, the change in the mentioned characteristics are significant but not so drastic. The same is true if two monatomic gases are used as plasma gas and their ratios changed. For the torch described in table 1, simulations are carried out with nitrogen–oxygen mixtures in the ratios of 80 : 20 and 20 : 80. Differences in axial variation of potential, velocity and temperature profiles at the exit are presented in figure 9. It is observed that as oxygen concentration increases, arc voltage decreases and peaks in the velocity and temperature profiles at the exits also decrease.

3.5 *Torch nozzle design for improved plasma processing*

The effects of nozzle design on the plasma characteristics are investigated in this section. Such studies are important primarily for obtaining spray coatings of greater homogeneity, density, increased spraying efficiencies and better process economies. Comparison is made between a standard straight nozzle of 10 mm ID and a converging diverging nozzle (Laval nozzle) of 5 mm IED (inner exit diameter) and 10 mm OED (outer exit diameter). Simulated results for a straight nozzle and a Laval nozzle torch of the same exit diameter and operating at the same arc current (400 A) with same plasma gas (N_2–O_2 mixture at a ratio of 80 : 20) are presented in figures 10a–10f. It has been observed that there is a drastic change in the flow field and a significant change in the temperature field. Higher velocity field distributed over a wider area superimposed with a more uniform temperature field results in better control of particle trajectories for Laval nozzle. Consequently, one gets higher deposition efficiencies and denser coatings. Properties of the plasma sprayed deposits get significantly influenced by the effects of the observed modifications in the temperature and associated electron density fields.

4. Conclusion

Evolving mechanical design of a plasma torch from numerical simulation is presented in this article. Starting from the basic governing equations, numerical recipe for predicting the characteristics of a designed plasma torch is discussed with specific examples of a plasma torch operating with a mixture of molecular gases like nitrogen and oxygen. Various torch characteristics such as, flow field, temperature field, electrical characteristics, thermal load to different components and efficiency of the plasma torch are directly obtained from numerical simulation. Effects of different nozzle designs and variations in gas compositions are also presented to establish the effectiveness and importance of simulation studies. While actual experiments are indispensable, numerical simulation for

obtaining optimum design parameter of a plasma device is an extremely time saving and cost-effective solution.

Acknowledgements

The authors would like to thank Dr L M Gantayet, Director, BTDG, BARC, for his encouragement and interest in this work.

References

[1] E Pfender, *Plasma Chem. Plasma Process.* **19**, 1 (1999)
[2] P Castrucci *et al*, *Thin Solid Films* **508**, 226 (2006)
[3] C Balasubramanian *et al*, *Nanotechnology* **15**, 370 (2004)
[4] J Heberlein and A B Murphy, *J. Phys. D: Appl. Phys.* **41**, 053001 (2008)
[5] R J Munz and G Q Chen, *J. Nucl. Mater.* **161**, 140 (1989)
[6] Q Zhang *et al*, *Appl. Energy* **98**, 219 (2012)
[7] R Ichiki *et al*, *Mater. Lett.* **71**, 134 (2012)
[8] F Lu *et al*, *Adv. Mater. Res.* **211**, 766 (2011)
[9] Y Katamune *et al*, *Jpn J. Appl. Phys.* **51**, 068002 (2012)
[10] S Furukawa *et al*, *J. Nucl. Sci. Technol.* **46**, 973 (2009)
[11] Y Kusano *et al*, *Surface & Coatings Technol.* **202**, 5579 (2008)
[12] T K Bose and R V Seeniraj, *Plasma Phys. Controlled Fusion* **26**, 1163 (1984)
[13] E Pfender, *Pure Appl. Chem.* **57**, 1179 (1985)
[14] A H Dilawari *et al*, *Plasma Chem. Plasma Process.* **10**, 321 (1990)
[15] J J Lowke, P Kovitya and H P Schmidt, *J. Phys. D: Appl. Phys.* **25**, 1600 (1992)
[16] J Haidar, *J. Phys. D: Appl. Phys.* **32**, 263 (1999)
[17] X Chen and H P Li, *Surface and Coatings Technol.* **171**, 124 (2003)
[18] A B Murphy *et al*, *High Temp. Mater. Process.* **12**, 255 (2008)
[19] G Yang, P Cronin, J V Heberlein and E Pfender, *J. Phys. D: Appl. Phys.* **39**, 2764 (2006)
[20] S Ghorui, S N Sahasrabudhe and A K Das, *J. Phys. D: Appl. Phys.* **43**, 245201 (2010)
[21] S Ghorui, J V R Heberlein and E Pfender, *J Phys D: Appl Phys.* **40**, 1966 (2007)
[22] S Ghorui, J V R Heberlein and E Pfender, *Plasma Chem. Plasma Process.* **28**, 553 (2008)
[23] V Colombo, E Ghedini and P Sanibondi, *Prog. Nucl. Energy* **50**, 921 (2008)
[24] B Gross, B Grycz and K Miklossy, *Plasma technology* (Iliffe Books, London, 1969)
[25] S V Dresvin, *Physics and technology of low temperature plasmas* (Atomizdat, Moscow, 1972)
[26] E Pfender, *Gaseous electronics* edited by M N Hirsh and H J Oskam (Academic Press, New York, 1978)
[27] O P Solonenko and M F Zhukov, *Thermal plasma and new materials technology* (Cambridge Interscience Publishing, Cambridge, 1995)
[28] A V Engel, *Electric plasmas: Their nature and uses* (Taylor and Francis, London, 1983)
[29] V Colombo *et al*, *Plasma Sources Sci. Technol.* **19**, 065025 (2010)
[30] J O Hirschfelder, C F Kurtis and R B Bird, *Molecular theory of gases and liquids*, 2nd edn. (Wiley, New York, 1964)
[31] S Chapman and T G Cowling, *The mathematical theory of transport processes in gases* (North-Holland, Amsterdam, 1972)
[32] M Capitelli, G Colonna, C Gorse and A D'Angola, *Eur. Phys. J. D* **11**, 279 (2000)
[33] M Capitelli, C Gorse and S Longo, *J. Thermo. Phys. Heat Transfer* **14**, 259 (2000)
[34] S V Patankar, *Numerical heat transfer and fluid flow* (McGraw-Hill, New York, 1980)